

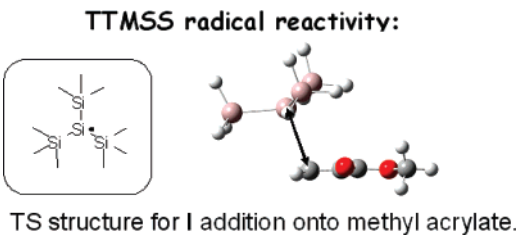
Tris(trimethylsilyl)silane (TTMSS)-Derived Radical Reactivity toward Alkenes: A Combined Quantum Mechanical and Laser Flash Photolysis Study

Jacques Lalevée,* Xavier Allonas, and Jean Pierre Fouassier

Department of Photochemistry, Ecole Nationale Supérieure de Chimie de Mulhouse, 3 rue Alfred Werner, 68093 Mulhouse Cedex, France

j.lalevee@uha.fr

Received March 29, 2007



The reactivity of the tris(trimethylsilyl)silane (TTMSS)-derived radical is studied through an approach combining laser flash photolysis and quantum mechanical calculations. The results obtained for TTMSS are compared both to a classical silyl radical derived from triethylsilane and to a previously studied carbon-centered structure. Different worthwhile results are obtained: (i) the addition and hydrogen abstraction rate constants are directly measured, (ii) the high reactivity and the low selectivity of TTMSS toward the addition to alkenes are perfectly explained by antagonist polar and enthalpy effects, (iii) efficient hydrogen abstraction reactions from antioxidants such as vitamin E are observed, and (iv) TTMSS is seen to also act as an efficient initiator for the polymerization of an acrylate monomer.

Introduction

The search for new radical structures having enhanced properties for the addition reaction to alkenes can be of interest in organic synthesis or polymer chemistry. Particularly, the hydrosilylation process, described by addition of silicon hydrides to carbon–carbon double bonds, presents a huge interest for the organosilicon compounds production and is used nowadays as a fundamental and elegant methodology for academic and industrial synthetic chemistry applications.^{1–2} Among the different structures proposed so far, tris(trimethylsilyl)silane (TTMSS) is now well recognized as an interesting structure for these reactions and can also be used as a radical base reducing agent in organic synthesis.^{1,3,4a,5–6} Nowadays, the attractiveness of

TTMSS (in replacement of tin derivatives) in radical organic chemistry is largely associated with the synthesis of camptothecin derivatives, this compound being of much interest for cancer treatments.^{1,4}

For a better understanding of the TTMSS reactivity, two items of great interest should be investigated: (i) the addition of silyl radicals to alkenes and (ii) their hydrogen abstraction ability from phenolic compounds. The TTMSS reactivity is actually mainly based on indirect measurements. The available addition rate constants are scant; the main values are gathered in ref 1. Moreover, no quantum mechanical calculations have been reported for TTMSS despite the great interest of this approach for a better understanding and improvement of the associated chemical processes.

In this paper, we will compare the reactivity of the silyl radical **I** derived from TTMSS to that of classical silicon-centered structure **II** derived from triethylsilane TES (Scheme 1). Radical **III** is used as a reference structure for the discussion since a

(1) Chatgilialoglu, C. *Organosilanes in Radical Chemistry*; Wiley: Chichester, 2004.

(2) *Comprehensive Handbook on Hydrosilylation*; Marciniec, B., Ed.; Pergamon: Oxford, 1992.

(3) Chatgilialoglu, C.; Griller, D.; Lesage, M. *J. Org. Chem.* **1988**, *53*, 3642–3644.

(4) (a) Ballestri, M.; Chatgilialoglu, C.; Clark, K. B.; Griller, D.; Giese, B.; Kopping, B. *J. Org. Chem.* **1991**, *56*, 678–683. (b) Yabu, K.; Masumoto, S.; Yamasaki, S.; Hamashima, Y.; Kanai, M.; Du, W.; Curran, D. P.; Shibasaki, M. *J. Am. Chem. Soc.* **2001**, *123*, 9908–9909.

(5) Chatgilialoglu, C.; Guerrini, A.; Lucarini, M. *J. Org. Chem.* **1992**, *57*, 3405–3409.

(6) Kopping, B.; Chatgilialoglu, C.; Zehnder, M.; Giese, B. *J. Org. Chem.* **1992**, *57*, 3994–4000.

SCHEME 1

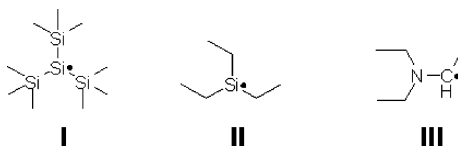


TABLE 1. Rate Constants Characterizing Silyl Radical Formation in Benzene

	$k_H (t\text{-Bu-O}^\bullet)$ $10^7 \text{ M}^{-1} \text{ s}^{-1}$	$k_H (^3\text{BP})$ $10^7 \text{ M}^{-1} \text{ s}^{-1}$	$\phi \kappa^\bullet$
TTMSS	8.5 ^a (11) ^b	10.2	0.95
TES	1.0 ^a (0.57) ^b	0.83	0.81

^a At 25 °C; the error bar is about 10%. ^b From ref 1 at 27 °C.

large variety of rate constants and quantum mechanical calculations are now available for this compound.^{7–9} Two reactions will be investigated: (i) the addition to double bonds having very different electron acceptor/donor properties such as vinyl ethyl ether, vinyl acetate, methyl acrylate, acrylonitrile, vinyl-carbazole, and styrene and (ii) the hydrogen abstraction using two different phenols as hydrogen donor compounds such as hydroquinone methyl ether (HQME) and vitamin E, two compounds that are often encountered, for example, as stabilizers in polymer chemistry or antioxidants in biological systems, respectively.²⁶ These reactions will be studied by laser flash photolysis and quantum mechanical calculations.

Results and Discussions

1. Formation of Silyl Radicals. The generation of silyl radicals can arise in two ways. The first one is based in Scheme 2 (Experimental Section). The interaction of the *tert*-butoxyl radical with TTMSS yields the silyl radical whose absorption (known as usually weak for $\lambda > 300 \text{ nm}$ ^{10–11}) can however be followed at 320 nm; the rise time of this absorption allows the evaluation of the interaction rate constants by a Stern–Volmer approach (Table 1). The second way involves an interaction with a ketone triplet state such as benzophenone (BP) that leads to a hydrogen abstraction, which generates ketyl and silyl radicals. In that case, the ketyl radicals of BP are easily observed at 545 nm. The observed rate constants as well as the ketyl radicals quantum yields ($\phi \kappa^\bullet$), which is also equal to the silyl radicals quantum yields, are gathered in Table 1.

Both processes appear as efficient and very high quantum yields for silyl radicals are observed with ³BP. The higher reactivity of **I** can be ascribed to its lower Si–H bond dissociation energy (see below). For *t*-Bu-O[•], the absolute values

(7) Lalevée, J.; Allonas, X.; Fouassier, J. P. *J. Am. Chem. Soc.* **2003**, *125*, 9377–9380.

(8) Lalevée, J.; Allonas, X.; Fouassier, J. P. *J. Phys. Chem. A* **2004**, *108*, 4326–4334.

(9) Lalevée, J.; Allonas, X.; Fouassier, J. P. *J. Org. Chem.* **2006**, *71*, 9723.

(10) (a) Chatgilialoglu, C.; Ingold, K. U.; Scaiano, J. C. *J. Am. Chem. Soc.* **1983**, *105*, 3292–3296. (b) Chatgilialoglu, C.; Ingold, K. U.; Scaiano, J. C. *J. Am. Chem. Soc.* **1982**, *104*, 5119–5123. (c) Chatgilialoglu, C.; Rossini, S. *Bull. Soc. Chim. Fr.* **1988**, *2*, 298.

(11) (a) Chatgilialoglu, C.; Guerra, M.; Guerrini, A.; Seconi, G.; Clark, K. B.; Griller, D.; Kanabus-Kaminska, J.; Martinho-Simoes, J. A. *J. Org. Chem.* **1992**, *57*, 2427. (b) Chatgilialoglu, C.; Ingold, K. U.; Lusztyk, J.; Nazran, A. S.; Scaiano, J. C. *Organometallics* **1983**, *2*, 1332. (c) Chatgilialoglu, C.; Dickhaut, J.; Giese, B. *J. Org. Chem.* **1991**, *56*, 6399–6403. (d) Chatgilialoglu, C.; Ferreri, C.; Lucarini, M.; Pedrelli, P.; Pedulli, G. F. *Organometallics* **1995**, *14*, 2672–2676.

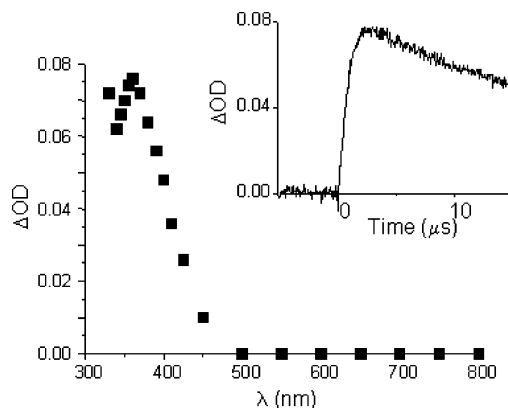


FIGURE 1. Transient absorption spectrum for the radical adduct in the **IMA** system ($t = 900$ ns); (insert) kinetic recorded at 360 nm [TTMSS] = 0.21 M; [MA] = 0.072 M (the rising time for the adduct radical is 610 ns).

found are in good agreement with previous works.¹ However, TTMSS is found 8.5 times faster than TES, whereas from the literature, the reactivity ratio was about 20. This difference can be ascribed to the indirect method used previously, which contains probably a slightly higher experimental error.

A more refined analysis of the mechanisms involved in these reactions, which are beyond the scope of the present paper, are however basically interesting and will be examined in detail in a forthcoming paper using a larger range of silanes.

For a detailed analysis of **I** and **II** reactivity, only the first method using *tert*-butoxyl radical will be used since the observation of the benzophenone ketyl radical in the second approach prevents the observation of both the silyl radical and the potential adduct species.

2. Addition Reaction: High Reactivity of Silyl Radicals toward Alkenes. Laser flash photolysis makes it possible to monitor the relatively intense absorption of the radical adducts above 320 nm (Figure 1). The addition rate constants are thus calculated from a classical Stern–Volmer analysis based on the rising time of these adducts, which corresponds to the decay time of the precursor radical (Figure 2). The alkene concentration ranges used have been changed for the different rate constants: in all cases, the rising time has been varied from $t \gg 10 \mu\text{s}$ to $t < 1 \mu\text{s}$.

The addition rate constants of **I** and **II** for different alkenes are gathered in Table 2. For some values, a comparison can be made with values previously measured and a very good agreement is found.¹ For **III**, the experimental data gained from ref 9 showed that the rate constants are high for AN and MA ($> 3 \times 10^7 \text{ M}^{-1} \text{ s}^{-1}$) and very low for VA, VC, and VE ($< 5 \times 10^4 \text{ M}^{-1} \text{ s}^{-1}$). The **III**/STY rate constant ($1.1 \times 10^6 \text{ M}^{-1} \text{ s}^{-1}$) was evaluated here through the direct observation of **III** at 340 nm.

For a better characterization of the **I**–**II** reactivity, quantum mechanical calculations were carried out. The values of the ionization potentials, the electronic affinities, and the electronegativities are reported in Table 3. For the silyl radicals, the agreement between the calculated and the experimental data is good, confirming the ability of the selected DFT procedure to describe these structures (for **I** and **II**, EA of 1.77 and 0.94 eV are calculated and can be compared to the experimental data of 2.03 and 0.97 eV, respectively).

For the different investigated alkenes, the striking feature is that the k_a values for **I** and **II** are always found higher than for

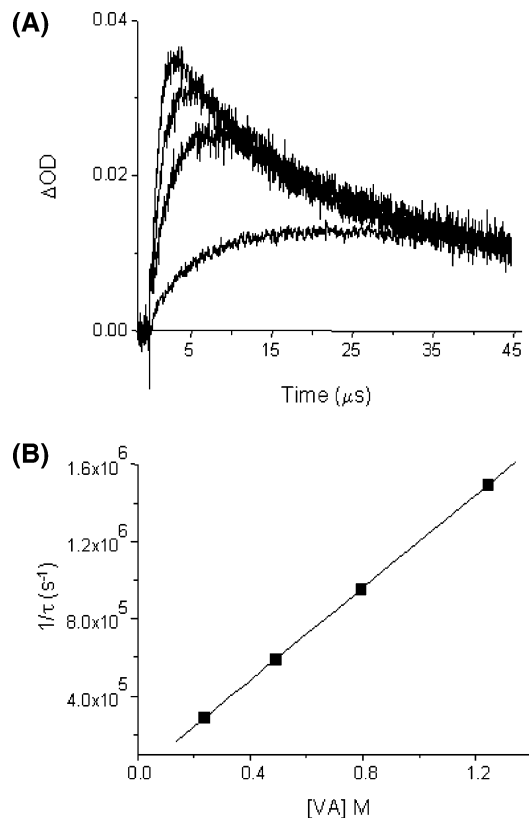


FIGURE 2. (A) Kinetics recorded at 360 nm for the radical adduct in the **I**/VA system $[TTMSS] = 0.2$ M; $[VA] = 0.23; 0.49; 0.79; 1.24$ M, respectively. (B) The associated Stern–Volmer treatment for the **I**/VA addition rate constant determination.

TABLE 2. Rate Constants (k_a) for Addition Reactions of **I and **II** to Different Alkenes**

alkene	k_a ($M^{-1}s^{-1}$)	
	I	II
STY	5.1×10^7 (5.9×10^7) ^a	2.1×10^8 (2.2×10^8) ^a
AN	5.1×10^7 (6.3×10^7) ^a	1.1×10^9 (1.1×10^9) ^a
MA	2.2×10^7 (9.7×10^7) ^a	2.4×10^8
VA	1.2×10^6	3.5×10^6
VC	5.1×10^6	8×10^7
VE	2.1×10^5	9×10^4

^a From ref 1.

TABLE 3. Electronic Properties for Alkenes and Radicals Used

	IP (eV) ^a	EA (eV) ^a	χ (eV) ^a
AN	10.5 (10.9) ^c	0.12 (-0.2) ^c	5.3 (5.4) ^e
MA	9.64 (9.9) ^c	0.09 (-0.5) ^c	4.9 (4.7) ^e
VA	8.91 (9.2) ^c	-0.48 (-1.2) ^c	4.2 (4.0) ^e
STY	8.07	-0.13	3.97
VC	7.18	-0.00	3.6
VE	8.31 (8.8) ^c	-1.5 (-2.2) ^c	3.4 (3.3) ^e
I	6.36	1.77 (2.03) ^b	4.06
II	6.1 (6.20) ^{b,d}	0.94 (0.97) ^{b,d}	3.52 (3.58) ^e

^a At UB3LYP/6-31+G* and ZPE corrected. ^b In parentheses are the experimental data from ref 1. ^c From ref 12. ^d For trimethylsilane.¹ ^e From the experimental data and eq 1. For **III**, IP = 4.96 eV, EA = -0.35 eV, χ = 2.31 eV.⁹

III, which was already considered as a highly reactive structure.⁷⁻⁹ The substrates range from alkenes bearing a withdrawing substituent to electron rich alkenes; therefore, silyl radicals appear as highly efficient and exhibit a rather low selectivity

TABLE 4. Thermodynamical Data and Transition State Properties for the Different Radical/alkene Systems. See Text.

system	ΔH_R^a (kJ/mol)	$\delta^{\text{TS}}b$	$d(\text{Si}-\text{C})^a$ (Å)	barrier ^b (kJ/mol)	$\log(k_{\text{a,cal}})$
I /AN	-70.1	0.04	2.900	10.5	5.7
I /MA	-62.5	0.025	2.897	10.8	4.9
I /VA	-36.4	-0.015	2.687	19.6	3.6
I /STY	-62.1	-0.03	2.830	12.3	5.0
I /VC	-33.5	-0.05	2.695	16.5	4.3
I /VE	-30.5	-0.08	2.671	20.6	2.9
II /AN	-120.9	0.05	3.207	3.1	7.1
II /MA	-115.3	0.04	3.143	3.7	6.7
II /VA	-86.4	0.015	2.84	18.7	4.2
II /STY	-121.1	-0.01	3.12	7.5	6.15
II /VC	-84.2	-0.025	2.822	12.1	4.8
II /VE	-83.8	-0.03	2.811	21.8	2.9

^a UB3LYP/6-31G* and ZPE corrected at 6-31G* level. ^b Single points at UB3LYP/6-311++G** level on the geometry determined at 6-31G* level, ZPE corrected at 6-31G* level.

toward the addition process. For the carbon-centered structure **III**, k_a decreases by at least a factor of 1000 from AN to VA; for **I** and **II**, the factor is only 50 and 300, respectively (**I** is found as the less selective one with a change lower than a factor of 200 on the complete scale of double bonds). This remarkable behavior of the silyl radicals is compared to the carbon-centered structures, which are usually highly selective.¹² For example, **III** exhibits an enhanced reactivity toward electron-deficient alkenes (particularly for monomers exhibiting $\chi > 4.5$ eV; $k_a > 3 \times 10^7 M^{-1} s^{-1}$) and a very low reactivity toward electron-rich structures ($k_a \ll 5 \times 10^4 M^{-1} s^{-1}$).⁹ All of the interactions with STY are rather high and do not follow the usual trend with the χ parameter: STY is a particular double bond because of the involvement of the π electrons of the phenyl ring and its low EA.¹²

The different calculated parameters characterizing the addition process of **I** and **II** to the different alkenes (ΔH_R , δ^{TS} , and the barrier) and the calculated addition rate constants k_a are gathered in Table 4. For the investigated systems, only the experimental barrier for **II**/STY has been previously determined (5.75 kJ/mol).¹ This is in good agreement with the calculated value (7.5 kJ/mol), demonstrating the validity of the selected procedure to describe the addition process.

The calculated and experimental k_a values are compared in Figure 3 for **I** and **II**. A general agreement good enough to describe the experimental trend is noted; this was also observed previously for **III**.⁹ The calculated values are found systematically lower than the experimental ones by about 1–2 orders of magnitude. This kind of behavior has been recently observed for sulfur-centered radicals,^{9,13} and such a difference is known for other systems in the literature.^{12,14} This difference arises from the combination of two effects: (i) the TST approach does not explicitly take into account the low frequency torsional modes, which are considered as vibrations, and (ii) the solvent is not explicitly taken into account. However, keeping in mind the difficulties¹⁵ for an accurate determination of both the transition

(12) Fischer, H.; Radom, L. *Angew. Chem., Int. Ed.* **2001**, *40*, 1340–1371.

(13) Lalevée, J.; Morlet-Savary, F.; Allonas, X.; Fouassier, J. P. *J. Phys. Chem. A* **2006**, *110*, 11605–11612.

(14) Coote, M. L. *Macromolecules* **2004**, *37*, 5023–5031.

(15) (a) *Gaussian* 98, Revision A.11; Frisch, M. J.; Trucks, G. W.; Schlegel, H. B.; Scuseria, G. E.; Robb, M. A.; Cheeseman, J. R.; Zakrzewski, V. G.; Montgomery, J. A., Jr.; Stratmann, R. E.; Burant, J. C.; Dapprich, S.; Millam, J. M.; Daniels, A. D.; Kudin, K. N.; Strain, M. C.; Farkas, O.;

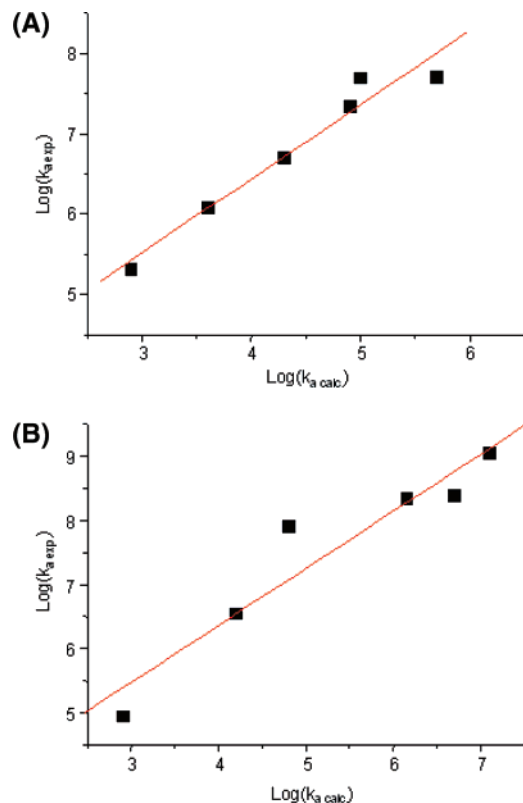


FIGURE 3. Plots of $\log(k_{a\text{exp}})$ versus $\log(k_{a\text{calc}})$ for **I** (A) and **II** (B).

state structure and the preexponential factor, the observed agreement can already be considered as good enough for an interpretation of the reactivity trends based on quantum mechanical calculations.

The addition reaction of a radical to a double bond (DB) is basically depicted by a state correlation diagram (SCD),^{12,16–20} which shows the potential energy profiles of the four lowest doublet configurations (the reactant ground state, the reactant excited state, and two charge-transfer configurations CTC R⁺/DB[–] and R[–]/DB⁺). In this approach, the barrier obviously decreases upon increasing the exothermicity. Moreover, the involvement of polar effects has been also found as greatly influencing the reaction through a decrease of the barrier when decreasing the CTC energies.^{8,12,21,22} A clear separation and a

Tomasi, J.; Barone, V.; Cossi, M.; Cammi, R.; Mennucci, B.; Pomelli, C.; Adamo, C.; Clifford, S.; Ochterski, J.; Petersson, G. A.; Ayala, P. Y.; Cui, Q.; Morokuma, K.; Salvador, P.; Dannenberg, J. J.; Malick, D. K.; Rabuck, A. D.; Raghavachari, K.; Foresman, J. B.; Cioslowski, J.; Ortiz, J. V.; Baboul, A. G.; Stefanov, B. B.; Liu, G.; Liashenko, A.; Piskorz, P.; Komaromi, I.; Gomperts, R.; Martin, R. L.; Fox, D. J.; Keith, T.; Al-Laham, M. A.; Peng, C. Y.; Nanayakkara, A.; Challacombe, M.; Gill, P. M. W.; Johnson, B.; Chen, W.; Wong, M. W.; Andres, J. L.; Gonzalez, C.; Head-Gordon, M.; Replogle, E. S.; Pople, J. A. Gaussian, Inc.: Pittsburgh, PA, 2001. (b) Foresman, J. B.; Frisch, A. In *Exploring Chemistry with Electronic Structure Methods*, 2nd ed.; Gaussian Inc.: Pittsburgh, PA, 1996.

(16) Tedder, J. M. *Angew. Chem., Int. Ed.* **1982**, *21*, 401–432.

(17) Shaik, S. S.; Shurki, A. *Angew. Chem., Int. Ed.* **1999**, *38*, 586–625.

(18) Shaik, S. S.; Canadell, E. *J. Am. Chem. Soc.* **1990**, *112*, 1446–1452.

(19) Wong, M. W.; Pross, A.; Radom, L. *J. Am. Chem. Soc.* **1994**, *116*, 6284–6292.

(20) Heberger, K.; Lopata, A. *J. Org. Chem.* **1998**, *63*, 8646–8653.

(21) Lalevée, J.; Allonas, X.; Fouassier, J. P. *Chem. Phys. Lett.* **2005**, *415*, 202–205.

(22) Lalevée, J.; Allonas, X.; Fouassier, J. P. *J. Org. Chem.* **2005**, *70*, 814–819.

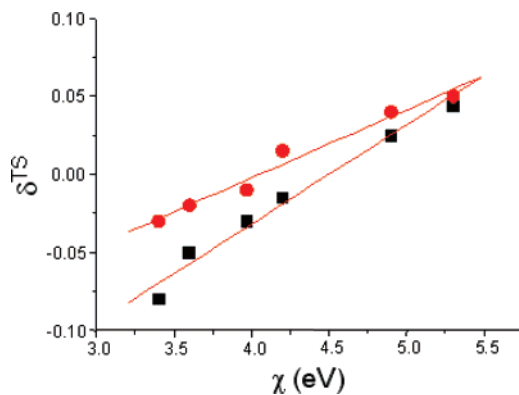


FIGURE 4. δ^{TS} versus χ of alkenes for **I** (square) and **II** (circle).

quantification of both polar and enthalpy factors were recently proposed for carbon-^{8,22} and sulfur-centered^{9,13} radicals. The reaction exothermicity and the participation of a charge transfer in the TS of the silyl radical addition are now evaluated.

Enthalpy Effect. For **I**, the exothermicity is systematically found to be about 50 kJ/mol lower than that for **II**. This result can be ascribed to the higher stabilization of **I** since the Si–H bond dissociation energies are 351.5 and 398 kJ/mol for TTMSS and TES, respectively.²³ As a higher exothermicity in the SCD approach leads to a higher reactivity, the higher reactivity of **II** can be ascribed to this effect.

Electron-withdrawing substituents generally increase χ_{DB} and stabilize the newly formed radical. Accordingly, ΔH_{R} was found to roughly depend on χ_{DB} for the different radical/alkene systems (except for STY as discussed above). This is in line with the fact that the reaction enthalpy and the electronic affinity EA_{DB} of the corresponding alkenes have been already shown to correlate when using other radicals,¹² the parameters χ_{DB} and EA_{DB} varying in a similar way.

The reaction exothermicity decreases in the series AN = STY > MA > VA > VC > VE. A decrease of 1 eV of the alkene absolute electronegativity χ_{DB} is associated to a lowering of about 30–40 kJ/mol of the reaction exothermicity. Therefore, the barrier is expected to increase with the decrease of the reaction exothermicity when going from AN to VE for a given radical. However, in the case of **I**, despite a strong decrease of the reaction exothermicity, the barrier change appears as fairly low. As a consequence, the enthalpy factor does not govern alone the barrier. For **II**, a decrease of the reaction exothermicity leads to a higher increase of the barrier. Concomitantly the experimental k_a values increase by a factor of 10 000 when going from VE to AN; in that case, the enthalpy mainly governs the barrier. The low change of the barrier for **I** and therefore its lower selectivity for the addition process can probably be ascribed to the participation of polar effects.

Polar Effect. The amounts of charge transfer in TS (which well characterize the polar effects^{8,12}) were calculated (Table 4). Polar effects are found higher for **I**, which appears to be more electrophilic with a net charge transfer from the double bond to the radical of 0.08 for VE instead of 0.03 for **II**/VE (Figure 4). For **II**, the δ^{TS} change is weaker demonstrating a lower influence of the polar effects than for **I**; this confirms that the **II** reactivity is mainly governed by ΔH_{R} (the participa-

(23) (a) Kanabus-Kaminska, J. M.; Hawari, J. A.; Griller, D.; Chatgilialoglu, C. *J. Am. Chem. Soc.* **1987**, *109*, 5267–5268. (b) Chatgilialoglu, C.; Newcomb, M. *Adv. Organomet. Chem.* **1999**, *44*, 67–112.

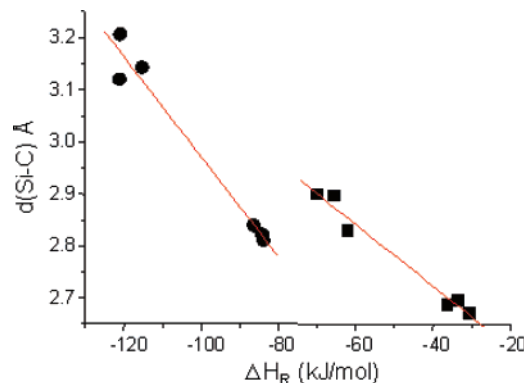


FIGURE 5. $d(\text{Si}-\text{C})$ in the TS structure versus ΔH_R for **I** (square) and **II** (circle).

tion of polar effects could probably explain why the addition of **II** to VC is higher than that to VA). Interestingly, the polar effect is very important for the **I**/electron-rich alkene systems leading for VE to a higher reactivity for **I** than for **II**. The low selectivity of **I** can be likely explained in term of an enthalpy effect decreasing from AN to VE, which is counterbalanced by a concomitant increase of the polar effects in this series. The situation is totally different when using an aminoalkyl radical. For **III**, strong polar effects were noted:^{8,21} the large positive δ^{TS} values (from 0.195, 0.189, 0.124, 0.131, 0.06 for AN, MA, VA, VC, VE, respectively; 0.106 for STY) support the fact that **III** behaves as a nucleophilic radical whatever the electron-rich or electron-deficient character of the monomer; the consequence is a drastic enhancement of the reactivity for alkenes bearing withdrawing substituents.

These behaviors are also reflected, as expected, by the radical absolute electronegativity χ_R (Figure 4). This is in agreement with the fact that the electronegativity difference (radical/alkene) corresponds to the driving factor of the charge transfer.^{8,24} For $\chi_R > \chi_M$, the charge transfer is observed from the alkene to the radical, and for $\chi_R < \chi_M$, from the radical to the alkene (Table 4).

TS Structures. The distances determined by quantum mechanical calculations in TS between the radical center (silicon atom) and the attacked carbon of the double bond $d(\text{Si}-\text{C})$ are gathered in Table 4. For **I** and **II**, the bond formation in the TS structure correlates with ΔH_R (Figure 5) in agreement with the Hammond's postulate, which states that the earliness of a transition structure is directly related to the reaction exothermicity. Interestingly, the points concerning **I** are still clearly above the correlation obtained for **II**, i.e., the structures of the corresponding TSs will be earlier for **I** than for **II** for a given exothermicity. This behavior can be ascribed to the polar effects that can also affect the TS structure, i.e., large polar effect leads to loser TS than expected from the enthalpy factor, as observed in other systems.²² Some steric effects associated with the crowded structure of **I** can also be expected.

3. Hydrogen Abstraction Reaction: Reactivity of Silyl Radicals toward Antioxidants. The rate constants, determined by a Stern–Volmer approach from the rising time of the well-known absorption of the phenoxy radical at 410 nm,²⁵ are gathered in Table 5. The Si–H bond dissociation energies

(24) Parr, R. G.; Pearson, R. G. *J. Am. Chem. Soc.* **1983**, *105*, 7512–7516.

(25) Das, P. K.; Encinas, M. V.; Steenken, S.; Scaiano, J. C. *J. Am. Chem. Soc.* **1981**, *103*, 4162–4166.

TABLE 5. Rate Constants of Interaction between Silyl Radicals and Phenols

	k_H (HQME) ($10^9 \text{ M}^{-1}\text{s}^{-1}$)	k_H (vitamin E) ($10^9 \text{ M}^{-1}\text{s}^{-1}$)	BDE (Si–H) (kJ/mol)
I	6.0	8.0	351.5 ^a
II	5.0	7.1	398 ^a

^a Reference 23.

(BDEs) for the investigated silanes have been previously determined by photoacoustic calorimetry (the revised values used were 351.5 and 398 kJ/mol for **I** and **II**, respectively)²³ as well as the O–H BDEs of HQME and vitamin E (346.5 and 327.3 kJ/mol, respectively).²⁶ It thus appears that **I**/vitamin E, **II**/HQME, and **II**/vitamin E interactions correspond to exothermic hydrogen transfer processes. Accordingly, very high rate constants are observed. Interestingly, for **I**/HQME, an almost athermic process is expected since $\text{BDE}(\text{O}-\text{H}) \approx \text{BDE}(\text{Si}-\text{H})$, but a high k_H is observed. It is reasonable to assume that a part of this reactivity is ascribable to the participation of the polar effects, the electronegativity of these structures (particularly **I**) being important. In the case of an aminoalkyl radical such as **III**, the rate constants for **III**/HQME and **III**/vitamin E interaction are $<1 \times 10^5 \text{ M}^{-1} \text{s}^{-1}$ and $0.6 \times 10^9 \text{ M}^{-1} \text{s}^{-1}$, respectively, although the BDE of **III** is 380 kJ/mol.²⁸ The polar effects still contribute but in the opposite direction as **III** is a nucleophilic radical and **I** an electrophilic radical. The high reactivity of **I** is also exemplified by the high rate constant measured here for the *tert*-butoxyl radical/vitamin E interaction ($2.3 \times 10^9 \text{ M}^{-1} \text{s}^{-1}$).

4. High Reactivity of I: Its Ability To Initiate a Polymerization Process. When using isopropylthioxanthone (ITX)/**I** as a photoinitiating system, the polymerization rate of the monofunctional acrylate monomer (MAM) is about one-half of that obtained in the presence of the ITX/ethylidemethylaminobenzoate (EDB) system (Supporting Information). This first result appears as highly interesting for the application of silane in photopolymerization reactions and once again unambiguously demonstrates its high reactivity.

Conclusion

In the present paper, the reactivity of silyl radicals toward both the addition onto alkenes and the hydrogen abstraction reaction was investigated. New rate constants of interaction as well as the first quantum mechanical calculations were reported. The principal findings are the following: (i) the high reactivity and the low selectivity of the TTMSS-derived radical toward the addition to alkenes are perfectly explained by antagonist polar and enthalpy effects, and this behavior is in full agreement with quantum mechanical calculations; (ii) efficient hydrogen abstraction reactions from antioxidants such as vitamin E are observed; and (iii) TTMSS can be considered as an efficient initiator for the polymerization of an acrylate monomer. This property is for the first time demonstrated.

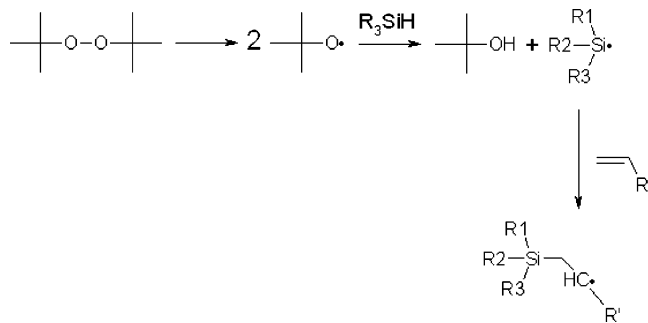
A general comparison of the silyl radicals with carbon-, germanium-, or tin-centered structures will be reported in

(26) Pedulli, G. F.; Lucarini, M.; Pedrielli, P. in *Free Radicals in Biology and Environment*; Minisci, F., Ed.; Kluwer Academic Publishers: Norwell, MA, 1997.

(27) Scaiano, J. C. *J. Phys. Chem.* **1981**, *85*, 2851–2855.

(28) Lalevée, J.; Allonas, X.; Fouassier, J. P. *J. Am. Chem. Soc.* **2002**, *124*, 9613–9621.

SCHEME 2



forthcoming studies, allowing a better understanding of the heteroatom effect on the associated reactivity.

In the same way, the polymerization-initiating properties of selected silyl radicals should be interesting in the polymer area, i.e., high polymerization rates can be achieved with the insertion of Si derivatives in the polymer matrix. This can be also useful for photografting applications on silicon surfaces, as well as in silicone polymer science.

Experimental Section

TTMSS, triethylsilane, triethylamine, and di-*tert*-butylperoxide were used with the best purity available. In the case of liquid monomers such as vinyl ethyl ether (VE), vinyl acetate (VA), methyl acrylate (MA), acrylonitrile (AN), and styrene (STY), the stabilizer (HQME) was removed by column purification. Vinylcarbazole (VC) was purified by recrystallization.

The silyl radicals were generated from a hydrogen transfer reaction between *tert*-butoxyl radical and the silane. Basically, the reaction consists in two consecutive steps as already proposed.^{10,21,27} The first step is the generation of a *tert*-butoxyl radical through the photochemical decomposition of di-*tert*-butylperoxide; the second step corresponds to a Si-H (**I** and **II**) or α (C-H) (**III**) hydrogen abstraction reaction from the silane and the amine, respectively, which generates the expected radical. Then, this radical adds to a double bond and forms a radical adduct (Scheme 2).

The addition and hydrogen abstraction rate constants were determined by nanosecond laser flash photolysis (LFP). The setup, based on a pulsed Nd:Yag laser (Powerlite 9010, Continuum) operating at 10 Hz and delivering nanosecond pulses at 355 nm, has been already described in detail (resolution time 10 ns).²⁸ The solvent used was di-*tert*-butylperoxide/benzene (50%/50%). A second way for silyl radicals formation consists in the interaction between the ketone (benzophenone, BP) triplet state and the silane (benzene as solvent); the ketyl radical quantum yield in the case of benzophenone was determined by a classical procedure.²⁸

For the film photopolymerization experiments, a monofunctional acrylate monomer (2-[(butylamino)carbonyl]oxy]ethyl acrylate or Genomer 1122 -Rahn) was used. The photoinitiating systems were ITX/TTMSS (1%/1% w/w) and ITX/ ethyldimethylaminobenzoate (EDB) (1%/1% w/w) as a reference. The formulation is exposed

to the monochromatic light at 366 nm of a Hamamatsu light source (L8252, 150 W). The rates of polymerization are calculated from the evolution of the double content as a function of time, followed by FT-IR (Supporting Information).²⁹

Computational Procedure

The computational procedure used to determine the parameters characterizing the reaction (exothermicity, barrier, etc.) has been already discussed in detail for carbon- and sulfur-centered radicals.^{8,9} Reactants, products, and transition states (TSs) were fully optimized in the density functional theory framework¹⁵ (hybrid functional B3LYP) allowing the determination of both the reaction enthalpy (ΔH_R) and the barrier. The amount of charge (δ^{TS}) transferred from the radical to the alkene in the TS structure was used to evidence polar effects.^{8,9}

The barrier corresponds to the energetic difference between TS and the reactants, taking into account the zero point energy correction. The activation energy (E_a^{TS}) of the addition reaction was obtained from the calculated barrier with addition of the RT term as usually done.^{13,30–32} The addition rate constants were also calculated through the determination of the preexponential factor in the Arrhenius equation by the activated complex theory.^{30,31} The harmonic oscillator approximation^{31,32} was adopted for the activation entropy calculations. This treatment, presented in detail in ref 13, was assumed to be accurate enough.³²

Adiabatic ionization potentials (IP) and adiabatic electron affinities (EA) characterizing the reactants were calcd

culated by the same procedure as previously.⁸ The electron-deficient or electron-rich character of the different alkenes is represented by their absolute electronegativity (χ) calculated from eq 1.^{22,24} The same procedure was used to obtain the absolute electronegativity (χ_R) of the radicals.

$$\chi = (IP + EA)/2 \quad (1)$$

Acknowledgment. The authors thank Dr. Nicolas Blanchard for interesting discussions on TTMSS applications in organic synthesis and the CINES (Centre Informatique National de l'Enseignement Supérieur) for the generous allocation of time on the IBM SPsupercomputer.

Supporting Information Available: Scheme of the alkenes investigated (S-2). Photopolymerization kinetics for (a) ITX/EDB (1%/1% w/w) system in Genomer 1122 and (b) ITX/TTMSS (1%/1% w/w) system in Genomer 1122. The polymerization kinetics were followed by real time FTIR as presented in ref 29. Complete TS geometries as coordinates (Gaussian 98–03). This material is available free of charge via the Internet at <http://pubs.acs.org>.

JO0706473

(29) Lalevée, J.; Allonas, X.; Jradi, S.; Fouassier, J. P. *Macromolecules* **2006**, *39*, 1872.

(30) Arnaud, R.; Subra, R.; Barone, V.; Lelj, F.; Olivella, S.; Solé, A.; Russo, N. *J. Chem. Soc., Perkin Trans. 2* **1986**, 1517–1524.

(31) Pacey, P. D. *J. Chem. Educ.* **1981**, *58*, 612–615.

(32) Coote, M. L.; Henry, D. J. *Macromolecules* **2005**, *38*, 5774–5779.